$\sigma_{33}(z) = \lambda_j/(\lambda_j + \mu_j)[\sigma_{tt}(z) + \sigma_{nn}(z)], \quad z \in B_j.$

In Eq. (3), $\sigma_{\alpha\beta}$ and $\varepsilon_{\alpha\beta}$ are the components of bulk stress and strain tensors, respectively, defined in the Cartesian coordinates (n, t) ($\boldsymbol{n}$ is a normal to S_j), and λ_j and μ_j are the Lame constants of the bulk phase B_j.

The conditions of mechanical equilibrium are formulated in the terms of the generalized Young–Laplace equation and in the case of simplified constitutive equations of Gurtin–Murdoch model can be written as

$$\sigma(\zeta_1) = \kappa(x_1)\sigma_s(x_1) - i\frac{1}{h}\frac{d\sigma_s(x_1)}{dx_1}, \quad \zeta_1 \in S_1, \tag{4}$$

$$\Delta\sigma(\zeta_2) = \sigma^+(\zeta_2) - \sigma^-(\zeta_2) = i\frac{d\tau_s(x_1)}{dx_1}, \quad \zeta_2 \in S_2, \tag{5}$$

where $\sigma_s(x_1) = \sigma^S_{tt}(\zeta_1)$ is the surface stress, $\tau_s(x_1) = \sigma^S_{tt}(\zeta_2)$ is the interfacial stress, $\sigma = \sigma_{nn} + i\sigma_{nt}$ is the complex stress vector, $\sigma^{\pm} = \lim_{z\to\zeta_2 \pm i0}\sigma(z)$, h and κ are the metric coefficient and local curvature of S_1, respectively.

At infinity, $\sigma_{\alpha\beta}$ $(\alpha, \beta = \{1,2\})$ in Cartesian coordinates (x_1, x_2) and the rotation angle of the material particle ω are specified as

$$\lim_{x_2\to-\infty}\sigma_{11} = \sigma_2, \quad \lim_{x_2\to-\infty}\sigma_{22} = \lim_{x_2\to-\infty}\sigma_{12} = \lim_{x_2\to-\infty}\omega = 0. \tag{6}$$

It should be noted that the longitudinal stress can be a result of the lattice mismatch between the film and substrate materials [22]. Although it may also be caused by other factors, such as mechanical loading.

Since the surface/interface and bulk phases are assumed to be coherent, the boundary conditions are as follows

$$\varepsilon^S_{tt}(\zeta_1) = \varepsilon_{tt}(\zeta_1), \quad \zeta_1 \in S_1, \quad \Delta u(\zeta_2) = u^+(\zeta_2) - u^-(\zeta_2) = 0, \quad \zeta_2 \in S_2, \tag{7}$$

where $u = u_1 + iu_2$ is complex displacement vector, u_1 and u_2 are displacements along axes (x_1, x_2) and $u^{\pm} = \lim_{z\to\zeta_2 \pm i0} u(z)$.

During stress relaxation, the relief of the film surface may change. It is necessary to define the dependence of the relief amplitude A on the time τ taking into account the surface diffusion and elastic deformation of film coating.

3. Linear stability analysis

It is assumed that the morphological evolution of the stressed film surface occurs due to the surface diffusion caused by the non-uniform distribution of the chemical potential along the surface. According to [23], the atomic flux along the film surface S_1 is proportional to the gradient of the chemical potential χ

$$J(\zeta, \tau) = -\frac{D_s C_s}{k_b T}\frac{\partial\chi(\zeta,\tau)}{\partial s}, \tag{8}$$

where D_s is the self-diffusivity coefficient; C_s is the number of diffusing atoms per unit area; k_b is the Boltzmann constant, T is the absolute temperature and s is arc length along S_1.

Following [24], the local chemical potential of the surface can be defined as

$$\chi(\zeta, \tau) = [U(\zeta, \tau) - \kappa(\zeta, \tau)U_s(\zeta, \tau)]\Omega, \tag{9}$$

where Ω is the atomic volume, U is the strain elastic energy density and U_s is the surface energy.

Considering atomic flow along the surface and taking into account mass conservation law we obtain the following evolution equation which gives the change of surface profile $g(x_1, \tau) = \varepsilon(\tau)f(x_1)$ with time

$$\frac{\partial g(x_1,\tau)}{\partial\tau} = K_s h(x_1, \tau)\frac{\partial^2}{\partial s^2}[U(\zeta, \tau) - \kappa(\zeta, \tau)U_s(\zeta, \tau)], \; K_s = D_s C_s \Omega^2/(k_b T). \tag{10}$$

To integrate the partial differential equation (10) and derive the stability conditions, the elastic strain energy U and surface energy U_s along the film surface should be determined.

The elastic strain energy U can be written as [25]

$$U = \frac{1}{2}\sigma_{\alpha\beta}\varepsilon_{\alpha\beta}, \tag{11}$$

where the summation is implied over repeated indices.

It is should be noted that in previous works aimed at studying the evolution of the surface microrelief, the effect of surface strains was assumed to be insignificant and the surface energy U_s was considered quantitatively equal to the residual surface stress γ_1^0. However, at the nanoscale, the effect of surface elasticity can be significant [6, 15]. So, in the case of a simplified Gurtin–Murdoch surface/interface elasticity model, the surface energy takes the form [26]

$$U_s = \gamma_1^0(1 + \varepsilon_{tt}^s) + \frac{1}{2}(\lambda_1^s + 2\mu_1^s - \gamma_1^0)\varepsilon_{tt}^s\varepsilon_{tt}^s. \tag{12}$$

Thus, to solve evolution equation (10) it is necessary to know the stress-strain state of the film/substrate system. To this end, we use the solution of the plane strain problem for the nanosized film/substrate system with undulated surface profile, which was proposed in [21]. In accordance with the mentioned above paper, the original boundary value problem (1) – (7) is reduced to the system of integral equations using the boundary perturbation technique, Goursat–Kolosov complex potentials, Muskhelishvili representations for stress components, and the superposition principle. Since we study a weak change of the surface relief, the components of the stress and the strain tensors of the bulk and surface phases are defined using the first-order approximation of the boundary perturbation method [21,27,28]

$$\sigma_{ij} = \sigma_{ij(0)} + \varepsilon\sigma_{ij(1)},\ \varepsilon_{ij} = \varepsilon_{ij(0)} + \varepsilon\varepsilon_{ij(1)}, \tag{13}$$
$$\sigma_{tt}^s = \sigma_{tt(0)}^s + \varepsilon\sigma_{tt(1)}^s,\ \varepsilon_{tt}^s = \varepsilon_{tt(0)}^s + \varepsilon\varepsilon_{tt(1)}^s.$$

Unfortunately, the expressions for the components $\sigma_{ij(0)}$, $\sigma_{ij(1)}$, $\varepsilon_{ij(0)}$, $\varepsilon_{ij(1)}$, $\sigma_{tt(0)}^s$, $\sigma_{tt(1)}^s$, $\varepsilon_{tt(0)}^s$, $\varepsilon_{tt(1)}^s$ are not given in the paper due to their enormous size, although the detailed algorithm for their construction can be found in [21].

The linearization in the space of the parameter ε for the metric coefficient h and the curvature κ can be written as

$$\kappa(x_1, \tau) = \varepsilon(\tau)f''(x_1), \quad h(x_1, \tau) = 1. \tag{14}$$

Substituting (11) – (14) into (10), we obtain an ordinary differential equation the solution of which gives the amplitude as a function of time, physical and geometrical parameters

$$\ln(A(\tau)/A_0) = R\left(a, h_f, \lambda_1, \mu_1, \lambda_2, \mu_2, \lambda_1^s, \mu_1^s, \gamma_1^0, \lambda_2^s, \mu_2^s, \gamma_2^0, \sigma_2\right)\tau.$$

4. Numerical results

As an example, consider a metal-on-metal system. We assume that the Poisson coefficients of the film and substrate materials are equal, i.e. $\nu_1 = \nu_2$. This simplification allows us to analyze the effect of the substrate through only one parameter, coating-to-substrate stiffness ratio $r = \mu_1/\mu_2$. The bulk Lame parameters of the film coating correspond to aluminum and are equal to $\lambda_2 = 58.17$ GPa and $\mu_2 = 26.13$ GPa. To analyze the effect of surface/interface elasticity, we consider the surface/interface stiffness $M_j = \lambda_j^s + 2\mu_j^s$. The surface Lame parameters for aluminum with the crystal lattice orientation (111) are obtained by molecular modelling in [29] and correspond to the longitudinal surface stiffness $M_1 = 6.099$ N/m. However, the surface elastic constants depend on the crystallographic orientation and other factors [30], therefore, different values of surface/interface stiffness are considered below.

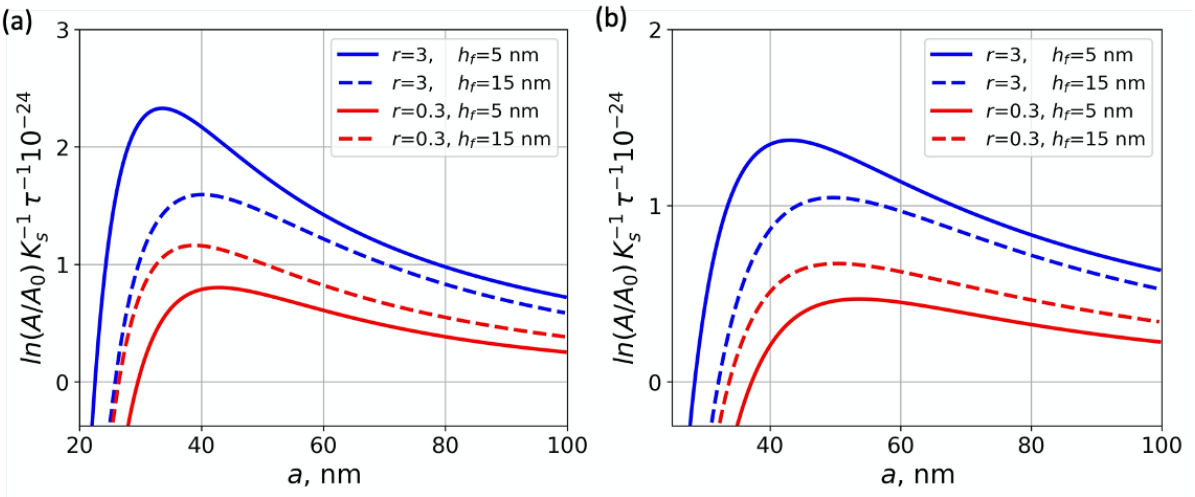

Fig. 2. The dependence of normalized amplitude change $A(\tau)/A_0$ on the perturbation wavelength a

Figure 2 shows the dependence of the normalized amplitude change $A(\tau)/A_0$ of the film surface relief on the perturbation wavelength a for different stiffness ratio $r = \{0.3;\ 3\}$ (red and blue lines, respectively), film thickness $h_f = \{5;\ 15\}$ nm (solid and dashed lines, respectively) and surface stiffness $M_1 = 6.099$ N/m (a) and $M_1 = 60$ N/m (b). We take an underestimated value of the residual surface stress to conduct a qualitative analysis of the influence of the surface elastic parameters. Thus, the residual surface stress is assumed to be equal to $\gamma_1^0 = 0.1$ N/m. The interface stiffness and residual stress are equal to $M_2 = 6.099$ N/m and $\gamma_2^0 = 1$ N/m, respectively. The critical wavelength a_{cr} corresponding to the thermodynamic equilibrium is found from the intersection of the lines with the abscissa. When the initial wavelength is less than the critical wavelength (i.e. $a < a_{cr}$), the perturbation amplitude decreases with time and the relief is smoothed out. If the initial wavelength is greater than the critical wavelength (i.e. $a > a_{cr}$), the undulation amplitude increases with time. The maximum amplitude change corresponds to a wavelength a_{max} which defines the unstable with the fastest growth rate. The wavelengths a_{cr} and a_{max} are presented in Table 1 and Table 2.

Table 1. The critical wavelength a_{cr} of film coating for various parameters

M_1, N/m	6.099	6.099	60	60
r	0.3	3	0.3	3
h_f, nm	a_{cr}, nm			
5	29.6	22.6	37.1	28.6
15	29.6	26.1	33.6	32.1

Table 2. The wavelength a_{max} of film coating for various parameters

M_1, N/m	6.099	6.099	60	60
r	0.3	3	0.3	3
h_f, nm	a_{max}, nm			
5	42.6	33.6	53.6	43.1
15	39.1	40.1	50.6	49.6

The critical wavelength is greater when the substrate is stiffer than the film (i.e., at $r < 1$). As can be seen from the results, the effect of the stiffness ratio increases when the thickness of the film coating decreases. When $M_1 = 6.099$ N/m and $h_f = 15$ nm, the influence of stiffness on the critical perturbation wavelength is insignificant. The wavelengths a_{max} increase with increasing surface stiffness M_1.

The effect of the interface stiffness M_2 and residual interface stress γ_2^0 on the morphological stability of the film surface has been also investigated. It was obtained that the critical wavelength of the film surface undulation marginally depends on interface parameters. In this regard, the interface stiffness and residual stress are assumed to be zero, i.e. $\gamma_2^0 = 0$ and $M_2 = 0$, in further analysis.

The dependence of the critical surface perturbation wavelength a_{cr} on surface stiffness M_1 and coating-to-substrate stiffness ratio r is shown in Fig. 3a and Fig. 3b, respectively. The critical wavelength a_{cr} increases with increasing surface stiffness M_1. The impact of the stiffness ratio is greater for films with smaller thickness and surface stiffness. The critical wavelength does not depend on the film thickness when the stiffness of the film and substrate materials are equal to each other (i.e., $r = 1$). In this case, the critical perturbation wavelengths correspond to an uncoated solid surface.

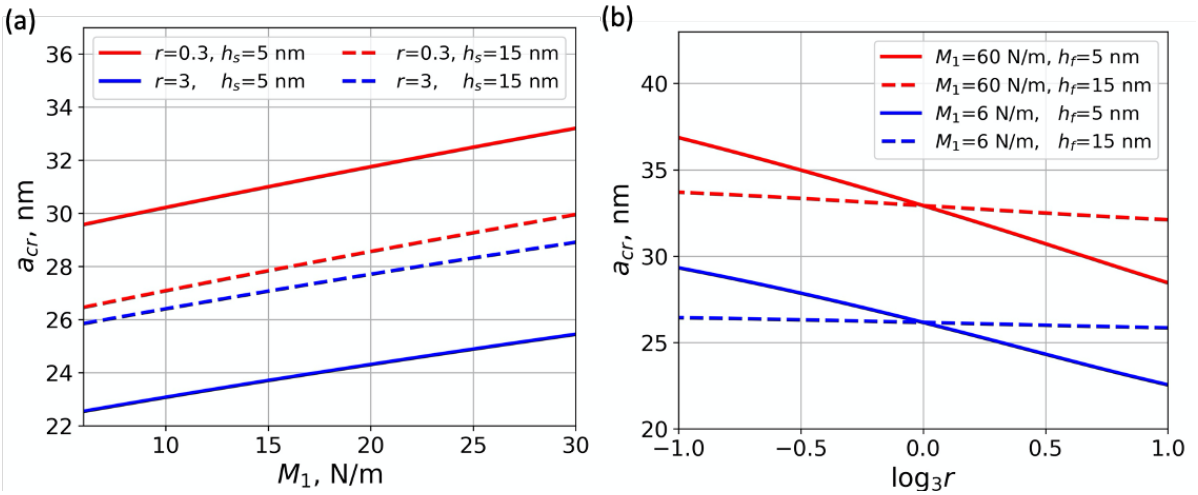

Fig. 3. The dependence of critical undulation wavelength a_{cr} on surface stiffness M_1 and stiffness ratio r

The dependence of critical undulation wavelength a_{cr} on residual surface stress γ_1^0 for $r = 0.3$ (a) and $r = 3$ (b) is plotted in Fig. 4. The critical wavelength a_{cr} increases with increasing of γ_1^0. In addition, the effect of residual surface stress on the morphological stability of the film surface is greater when the film is stiffer than the substrate (i.e., when $r = 0.3$). Also, the impact of the residual surface stress increases with decreasing film thickness in this case. If the substrate stiffness is less than the film stiffness (i.e. $r > 1$), the influence of the residual surface stress on critical wavelength is marginally dependent on film thickness and the surface stiffness.

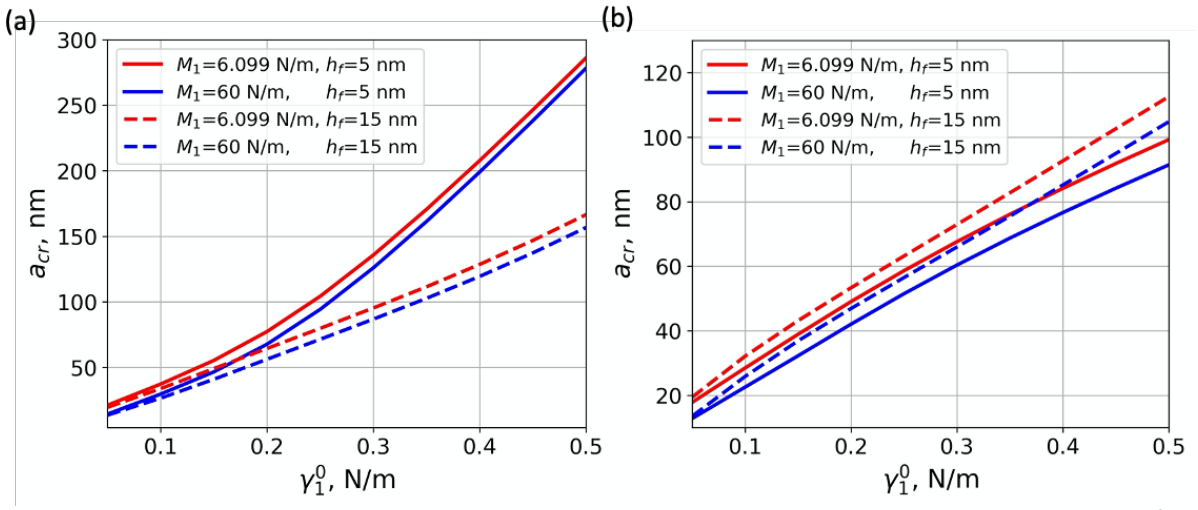

Fig. 4. The dependence of critical undulation wavelength a_{cr} on residual surface stress γ_1^0

Figure 5 demonstrates the dependence of critical undulation wavelength a_{cr} on its thickness h_f for different stiffness ratio $r = \{0.3, 3\}$ (blue and red lines, respectively), $M_1 = 6.099$ N/m (a) and $M_1 = 60$ N/m (b). The results show that the critical wavelength increase/decrease and tend to the critical wavelength corresponding to an uncoated solid surface with an increasing thickness of the film coating, which stiffness is greater/less than the substrate stiffness. The influence of the film thickness increases with an increasing surface stiffness M_1. The threshold thickness, exceeding which we can ignore the impact of a substrate, increases with increasing surface stiffness.

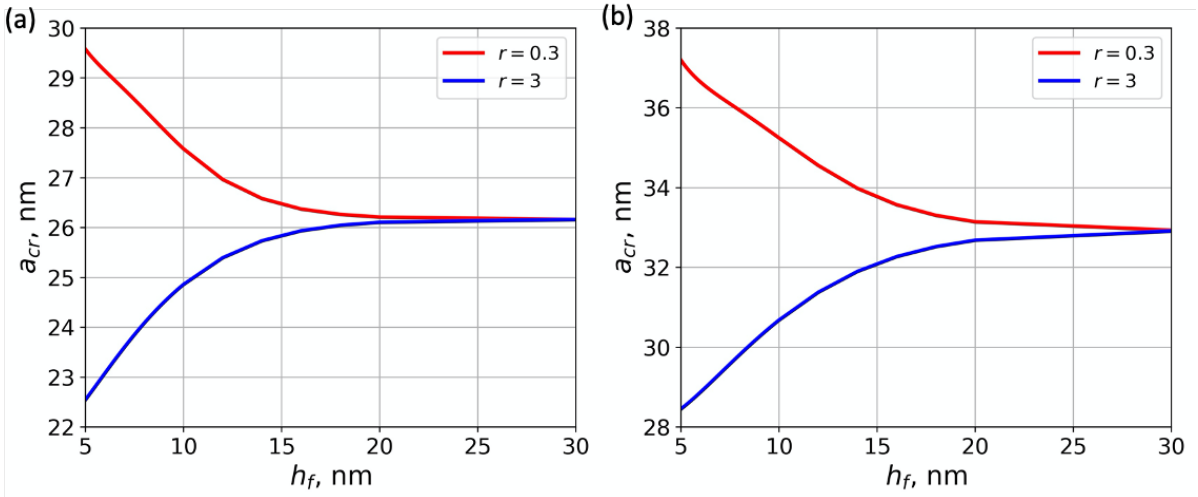

Fig. 5. The dependence of normalized deviation amplitude change $A(\tau)/A_0$ on the initial hole radius a

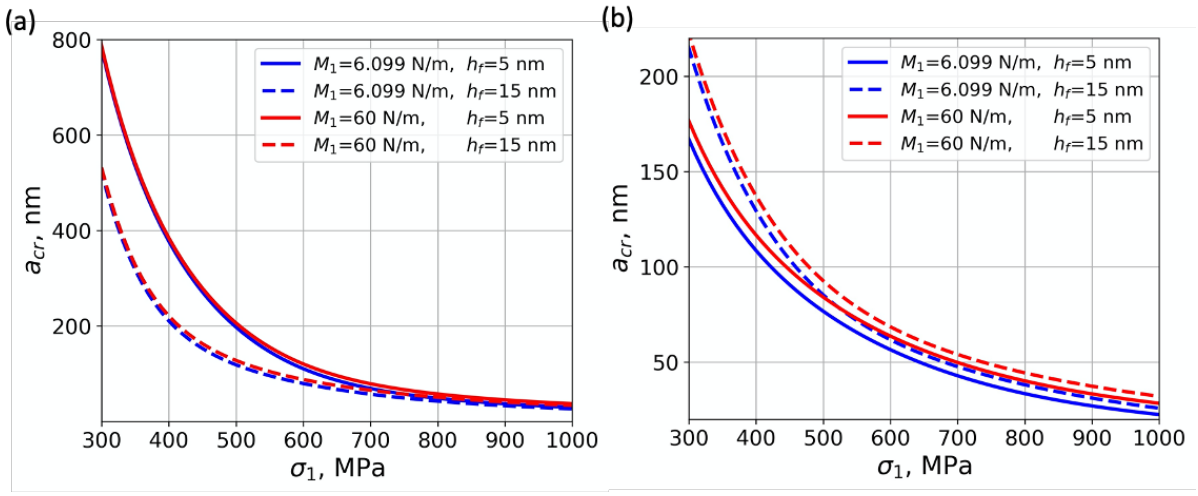

Fig. 6. The dependence of critical undulation wavelength a_{cr} on longitudinal stress σ_1

The dependence of critical undulation wavelength a_{cr} on longitudinal stress σ_1 for different surface stiffness $M_1 = \{6.099;\ 60\}$ N/m (blue and red lines, respectively), film thickness $h_f = \{5;\ 15\}$ nm (solid and dashed lines, respectively), and stiffness ratios $r = 0.3$ (a) and $r = 3$ (b) is shown in Fig. 6. One can see that the critical wavelengths decrease with increasing σ_1. The impact of surface stiffness increases with increasing longitudinal stress.

5. Conclusion

In this paper, a theoretical approach to the analysis of the surface morphological stability of the ultrathin film coating is developed. The impact of the surface/interface elastic properties is taken into account based on the Gurtin–Murdoch surface/interface elasticity model. It was assumed that the surface evolution of the film coating occurs due to surface diffusion driven by a nonuniform distribution of the chemical potential along the undulated surface. It was also postulated that the nonuniform distribution of the chemical potential along the surface is caused by changes in the stress field, surface energy, and surface curvature. The evolution of the surface relief was considered as a change in the amplitude of the periodic undulation.

The effect of coating-to-substrate stiffness ratio, elastic parameters of surface and interface, film thickness, residual surface/interface stress, and longitudinal stress were investigated. The following results were obtained:

– the interface stiffness and residual interface stress do not affect the morphological stability of the film coating surface;

– the critical perturbation wavelength increases with increasing surface stiffness, residual surface stress as well as with decreasing longitudinal stress and coating-to-substrate stiffness ratio;

– the effect of surface stiffness decreases with an increase in residual surface stress and a decrease in longitudinal stress;

– the critical perturbation wavelength increases/decreases with increasing film thickness when the film is stiffer/softer than the substrate;

– the impact of the substrate decreases with increasing film thickness;

– the threshold coating thickness, exceeding which it is possible to ignore the substrate, increases with an increase in surface stiffness and surface residual stress.

References

[1] Shang L, Xu B, Ma S, Liu Q, Ouyang H, Shan H, Hao X, Han B. The Surface Morphology Evolution of GaN Nucleation Layer during Annealing and Its Influence on the Crystal Quality of GaN Films. *Coatings.* 2021;11(2): 188.

[2] Wei L, Chunlei S, Miao C, Xiaosong Z, Xinggui L. The surface morphology evolution of ZrSi2 films under different substrate temperature. *Materials Research Express.* 2019;6(11): 116458.

[3] Pronina Y, Maksimov A, Kachanov M. Crack approaching a domain having the same elastic properties but different fracture toughness: Crack deflection vs penetration. *International Journal of Engineering Science.* 2020;156: 103374.

[4] Colin J, Grilhe J, Junqua N. Morphological instabilities of a stressed pore channel. *Acta Materialia.* 1997;45: 3835-3841.

[5] Freund LB. Evolution of waviness on the surface of a strained elastic solid due to stress-driven diffusion. *International Journal of Solids and Structures.* 1995;28: 911-923.

[6] Duan HL, Weissmuller J, Wang Y. Instabilities of core-shell heterostructured cylinders due to diffusions and epitaxy: spheroidization and blossom of nanowires. *Journal of the Mechanics and Physics of Solids.* 2008;56: 1831-1851.

[7] Cammarata RC. Surface and interface stress effects in thin films. *Progress in Surface Science.* 1994;46(1): 1-38.

[8] Fischer FD, Waitz T, Vollath D, Simha NK. On the role of surface energy and surface stress in phase-transforming nanoparticles. *Progress in Materials Science.* 2008;53: 481-527.

[9] Grekov MA, Kostyrko SA. Surface effects in an elastic solid with nanosized surface asperities. *International Journal of Solids and Structures.* 2016;96: 153-161.

[10] Shuvalov GM, Kostyrko SA. Surface self-organization in multilayer film coatings. *AIP Conference Proceedings.* 2017;1909: 020196.

[11] Chan SW, Wang W. Surface stress of nano-crystals. *Materials Chemistry and Physic.* 2021;273: 125091.

[12] Dai M, Schiavone P. Deformation-Induced Change in the Geometry of a General Material Surface and Its Relation to the Gurtin–Murdoch Model. *Journal of Applied Mechanics.* 2020;87(6): 061005

[13] Javili A, Bakiler AD. A displacement-based approach to geometric instabilities of a film on a substrate. *Mathematics and Mechanics of Solids.* 2019;24(9): 2999-3023.

[14] Mikhasev GI, Botogova MG, Eremeyev VA. On the influence of a surface roughness on propagation of anti-plane short-length localized waves in a medium with surface coating. *International Journal of Engineering Science.* 2021;158: 103428.

[15] Zhao X, Duddu R, Bordas S, Qu J. Effects of elastic strain energy and interfacial stress on the equilibrium morphology of misfit particles in heterogeneous solids. *Journal of the Mechanics and Physics of Solids.* 2013;61(6): 1433-1445.

[16] Gurtin ME, Murdoch AI. A continuum theory of elastic material surfaces. *Archive for Rational Mechanics and Analysis.* 1975;57(4): 291-323.

[17] Gurtin ME, Murdoch AI. Surface stress in solids. *International Journal of Solids and Structures.* 1978;14: 431-440.

[18] Panat R, Hsiaa KJ. Evolution of surface waviness in thin films via volume and surface diffusion. *Journal of Applied Physics.* 2005;97: 013521.

[19] Srolovitz DJ. On the stability of surfaces of stressed solids. *Acta Metallurgica.* 1989;37(2): 621-625.

[20] Ryu JJ, Shrotriya P. Influence of roughness on surface instability of medical grade cobalt–chromium alloy (CoCrMo) during contact corrosion–fatigue. *Applied Surface Science.* 2013;273: 536-541.

[21] Kostyrko SA, Altenbach H, Grekov MA. Stress concentration in ultra-thin coating with undulated surface profile. In: *Proceedings of the 7th International conference on coupled problems in science and engineering.* 2017. p.1183-1192.
[22] Gao H, Nix WD. Surface roughening of heteroepitaxial thin films. *Annual Review of Material Science.* 1999;29: 173-209.
[23] Asaro RJ, Tiller WA. Interface morphology development during stress-corrosion cracking: Part I. Via surface diffusion. *Metallurgical and Materials Transactions.* 1972;3: 1789-1796.
[24] Freund LB, Suresh S. *Thin film materials: stress, defect formation and surface evolution.* New York: Cambridge University Press; 2004.
[25] Novozhilov VV. *Theory of elasticity.* Oxford: Pergamon Press; 1961.
[26] Ru CQ. Simple geometrical explanation of Gurtin – Murdoch model of surface elasticity with clarification of its related versions. *Science China: Physics, Mechanics and Astronomy.* 2010;53(3): 536-544.
[27] Grekov MA, Vakaeva AB. The perturbation method in the problem on a nearly circular inclusion in an elastic body. In: *Proceedings of the 7th International Conference on Coupled Problems in Science and Engineering, COUPLED PROBLEMS 2017.* International Center for Numerical Methods in Engineering; 2017. p.963-971.
[28] Vakaeva AB, Krasnitckii SA, Grekov MA, Gutkin MY. Stress field in ceramic material containing threefold symmetry inhomogeneity *Journal of Materials Science.* 2020;55(22): 9311-9321.
[29] Miller RE, Shenoy VB. Size-dependent elastic properties of nanosized structural elements. *Nanotechnology.* 2000;11: 139-147.
[30] Shenoy VB. Atomistic calculations of elastic properties of metallic fcc crystal Surfaces. *Physical Review B.* 2005;71: 094104.

THE AUTHORS

Shuvalov G.M.
e-mail: g.shuvalov@spbu.ru
ORCID: 0000-0002-9039-4888

Kostyrko S.A.
e-mail: s.kostyrko@spbu.ru
ORCID: 0000-0003-3074-0969